This is an unedited, uncorrected chapter.

The final chapter will be available in time for fall.

NOTE: Figures and tables appear at the end of the chapter.

WEB CHAPTER W8

Axially Loaded Columns

W8.1 Stiffness of a Pin-ended Column as a Function of the Axial Load

Figure W8.1.1: Model for evaluating rotational stiffness of a column.

Consider the initially straight pin-ended column AB, subjected to an axial compressive force P, and two equal and opposite end moments M^o as shown in Fig. W8.1.1*a*. As a result of this loading, the column takes the deformed shape shown in Fig. W8.1.1*b*. The deflection at D, distance z from A, is indicated by u. Moment equilibrium of segment AD of this beam-column gives:

$$\Sigma (M)_D = 0 \quad \rightarrow \quad M = M^o + Pu \tag{W8.1.1}$$

The differential equation governing the deflected shape of the member is therefore given by:

$$-EI\,u'' = (M^o + Pu) \tag{W8.1.2}$$

By dividing both sides of this equation by EI and rearranging, we obtain:

$$u'' + \frac{P}{EI}u = -\frac{M^o}{EI} \quad \rightarrow \quad u'' + \alpha^2 u = -\frac{M^o}{EI} \qquad \text{(W8.1.3)}$$

where $\alpha^2 = P/EI$. The general solution of this second-order differential equation is given by:

$$u = C_1 \sin \alpha z + C_2 \cos \alpha z - \frac{M^o}{P} \qquad \text{(W8.1.4)}$$

Note that P (and hence α) and M^o are known quantities, while C_1 and C_2 are the integration constants to be determined from the boundary conditions. We have:

$$u = 0 \quad \text{at } z = 0 \qquad \rightarrow \quad C_2 = \frac{M^o}{P} \qquad \text{(W8.1.5)}$$

$$u = 0 \quad \text{at } z = L \qquad \rightarrow \quad C_1 \sin \alpha L + C_2 \cos \alpha L = \frac{M^o}{P}$$

$$\rightarrow \quad C_1 = \frac{M^o}{P}\frac{(1 - \cos \alpha L)}{\sin \alpha L} = \frac{M^o}{P} \tan \frac{\alpha L}{2} \qquad \text{(W8.1.6)}$$

The deflection u is therefore given by the expression:

$$u = \frac{M^o}{P}\left[\tan \frac{\alpha L}{2} \sin \alpha z + \cos \alpha z - 1\right] \qquad \text{(W8.1.7)}$$

The maximum deflection, δ, occurs at C, that is, at $z = L/2$, and is given by the expression:

$$\delta = \left(\frac{M^o}{P}\right)\left[\sec \frac{\alpha L}{2} - 1\right] \qquad \text{(W8.1.8)}$$

Also, since $P_E = \pi^2 EI/L^2$, $\alpha^2 L^2 = \dfrac{PL^2}{EI} = \pi^2 \dfrac{PL^2}{\pi^2 EI} = \pi^2 \dfrac{P}{P_E}$

Or,

$$\alpha L = \pi \sqrt{\frac{P}{P_E}} \tag{W8.1.9}$$

Now

$$sec \frac{\alpha L}{2} \rightarrow \infty \text{ as } \frac{\alpha L}{2} \rightarrow \frac{\pi}{2} \tag{W8.1.10}$$

From Eq. W8.1.8 we observe that the deflection δ therefore approaches infinity when αL approaches π, or as:

$$P \rightarrow P_E \tag{W8.1.11}$$

Hence, the Euler load P_E is also the maximum axial load the elastic, pin-ended member can sustain in the presence of the applied bending moments M^o.

By dividing both sides of Eq. W8.1.8 by L, and by dividing the numerator and denominator of the term within the first brackets by P_E, and substituting $\pi \sqrt{P/P_E}$ for αL, the maximum deflection δ given by Eq. W8.1.8 can be rewritten in the non-dimensional form:

$$\frac{\delta}{L} = \frac{\dfrac{M^o}{P_E L}}{\dfrac{P}{P_E}} \left[\sec \frac{\pi}{2} \sqrt{\frac{P}{P_E}} - 1 \right] \tag{W8.1.12}$$

Figure W8.1.2 gives a graphic representation of Eq. W8.1.12 for three different values of

$\frac{M^o}{P_E L}$.

Figure W8.1.2: Variation of deflection with axial load for a pin-ended column with end moments.

From Eq. W8.1.7 we obtain the slope at any point as:

$$u' = \frac{M^o}{P}\left[\alpha \tan\frac{\alpha L}{2} \cos \alpha z - \alpha \sin \alpha z\right] \qquad \text{(W8.1.13)}$$

In particular, the end slope is given by:

$$\theta_A = u'_{(z=0)} = \frac{M^o}{P} \alpha \tan\frac{\alpha L}{2} \qquad \text{(W8.1.14)}$$

The rotational stiffness k of the column with respect to end moments may be defined as the ratio of the applied moment M^o to end rotation θ_A. With the help of Eqs. W8.1.14 and W8.1.9, the rotational stiffness of the beam-column may be written as:

$$k = \frac{M^o}{\theta_A} = \frac{P}{\alpha \tan\frac{\alpha L}{2}} = \frac{EI\alpha}{\tan\frac{\alpha L}{2}} = \frac{2EI}{L}\frac{\frac{\alpha L}{2}}{\tan\frac{\alpha L}{2}}$$

Defining $k_o = (2EI/L)$ and utilizing Eq. W8.1.9,

$$\frac{k}{k_o} = \frac{\frac{\pi}{2}\sqrt{\frac{P}{P_E}}}{\tan\left(\frac{\pi}{2}\sqrt{\frac{P}{P_E}}\right)} \qquad \text{(W8.1.15)}$$

Here k_o is the rotational stiffness of the pin ended member under symmetric single curvature moments M^o, with $P = 0$. The variation of k/k_o with P/P_E is schematically shown in Fig. W8.1.3. It can be seen that the stiffness of the member reduces from k_o to zero as the axial load on the column increases from zero to the Euler load, P_E. The ***critical load of a column*** may thus be interpreted as that axial load at which the rotational stiffness of the column becomes zero.

Figure W8.1.3: Variation of rotational stiffness with axial load for a pin-ended column.

We observe from Eq. W8.1.15 that the stiffness of the isolated member considered is a function of the axial load only and is independent of the magnitude of the end moments M^o. For values of $P > P_E$, the stiffness k becomes negative, implying that the column must be provided with end moments that oppose the column end rotations. Such moments, called ***restraining moments***, are generally provided by suitably connecting the column ends to other members of the structure. It is only when such restraints are provided that any column will support an axial compressive load greater than its failure load as a pin- ended column (i.e., Euler load).

W8.2 Influence of Geometrical Imperfections on the Behavior of a Pin Ended Column

Figure W8.2.1: Imperfect pin-ended column.

Practical steel members almost always contain small, unavoidable geometrical imperfections as a result of rolling, fabrication, and erection. Such slight imperfections can be safely disregarded in tension members as the tensile loads will tend to straighten those members (see Section A5.1). On the other hand, slight imperfections in columns may be of major significance. In this section, the planar behavior of an imperfect column is studied by considering a pin-ended column with a centroidal axis that is initially bent (Fig. W8.2.1). The initial (unloaded) shape of such a column can be represented by the Fourier series:

$$u_o = \sum_{n=1}^{\infty} \delta_{on} \sin \frac{n\pi z}{L} \qquad \text{(W8.2.1)}$$

where u_o is the perpendicular distance from the chord joining the two ends of the member measured to the centroidal axis of the member.

The member is concentrically loaded by an end compressive force P, causing additional deflection u_a at section z. The total deflection is represented by $u = u_o + u_a$. Since bending strains are caused by the change in curvature, u_a'', and not by the total curvature, $u_o'' + u_a''$, the internal resisting moment at section z is:

$$M_{\text{int}} = -EI\, u_a'' \qquad \text{(W8.2.2)}$$

The externally applied bending moment at this section (Fig. W8.2.1) is:

$$M_{\text{ext}} = P(u_o + u_a) \qquad \text{(W8.2.3)}$$

The equilibrium equation obtained by combining Eqs. W8.2.2 and W8.2.3 is:

$$-EIu_a'' = P(u_o + u_a) \rightarrow u_a'' + \frac{P}{EI}u_a = -\frac{P}{EI}u_o \qquad \text{(W8.2.4)}$$

This is a nonhomogeneous, second-order differential equation with constant coefficients. The nonzero right hand side of Eq. W8.2.4 is simply a constant, and thus indicates that the imperfect column, unlike the perfect column, bends immediately upon application of axial load. That is, the solution of Eq. W8.2.4 can be obtained for all values of P rather than only for critical loads.

We can also use a Fourier series to describe the additional deflection, u_a, under the axial load P. Thus:

$$u_a = \sum_{n=1}^{\infty} \delta_{an} \sin\frac{n\pi z}{L} \qquad \text{(W8.2.5)}$$

Note that both Eqs. W8.2.1 and W8.2.5 satisfy the boundary conditions of the problem, namely, $u_o = u_a = 0$ at $z = 0$ and $z = L$. By substituting Eqs. W8.2.1 and W8.2.5 and the second derivative of Eq. W8.2.5 into Eq. W8.2.4, we obtain:

$$\sum_{n=1}^{\infty} \left[-\delta_{an} + \frac{PL^2}{n^2\pi^2 EI}\left(\delta_{on} + \delta_{an}\right)\right] \sin\frac{n\pi z}{L} = 0 \qquad \text{(W8.2.6)}$$

For this relation to be true for all values of P, the term within the bracket must equal to zero for all values of n. By introducing the relation for P_{crn} given in Eq. 8.4.12, we have:

(W8.2.7)

$$-\delta_{an} + \frac{P}{P_{crn}}(\delta_{on} + \delta_{an}) = 0 \rightarrow \delta_{an} = \frac{\delta_{on}}{\left[\frac{P_{crn}}{P} - 1\right]}$$

or

$$\delta_n = \delta_{on} + \delta_{an} = \frac{1}{\left[1 - \frac{P}{P_{crn}}\right]}\delta_{on} = A_{fn}\,\delta_{on} \qquad \text{(W8.2.8)}$$

The factors A_{fn}, by which the initial deflection components in the Fourier series are magnified due to the presence of the axial load P in the member, are called the ***amplification factors***. The total deflection at any distance z can now be written as:

$$u = \sum_{n=1}^{\infty} \delta_n \sin\frac{n\pi z}{L} = \sum_{n=1}^{\infty} \frac{\delta_{on}}{1 - \frac{P}{P_{crn}}} \sin\frac{n\pi z}{L} \qquad \text{(W8.2.9)}$$

$$= \frac{\delta_{o1}}{1 - \frac{P}{P_E}} \sin\frac{\pi z}{L} + \frac{\delta_{o2}}{1 - \frac{P}{2^2 P_E}} \sin\frac{2\pi z}{L} + \frac{\delta_{o3}}{1 - \frac{P}{3^2 P_E}} \sin\frac{3\pi z}{L} + \ldots$$

As the axial load P approaches the Euler load P_E, the amplification factors A_{fn} assume the following values:

n =	1	2	3	. . .	∞
$A_{fn} \rightarrow$	∞	$\frac{4}{3}$	$\frac{9}{8}$	. . .	1

From this we see that the first term of the Fourier series ($n = 1$) contributes most to the value of the resultant deflection. More generally, the value of n associated with the mode of buckling of a column when it is perfectly straight is also the value of n that has the most

influence in determining the resultant deflection of the imperfect column. Thus for the pin-ended column without intermediate bracing, we can conclude:

$$u_o = \delta_{o1} \sin\frac{\pi z}{L} \qquad \text{(W8.2.10}a\text{)}$$

$$u = \frac{\delta_{o1}}{\left(1 - \frac{P}{P_E}\right)} \sin\frac{\pi z}{L} \qquad \text{(W8.2.10}b\text{)}$$

$$\delta = \frac{\delta_o}{\left(1 - \frac{P}{P_E}\right)} \qquad \text{(W8.2.10}c\text{)}$$

For columns constrained to buckle in higher modes as shown in Figs. 8.4.3 *b* and *c*, *n* takes the values of 2 and 3 respectively. From Eq.W8.2.9 it can be seen that the 2nd and 3rd terms predominate in determining the respective values of the resultant deflections. Thus, of all the components of the Fourier series present in the initial geometrical imperfection of a column, only the component that corresponds to the buckling mode of the perfect column is of importance.

W8.3 Influence of End Fixity on Elastic Buckling of a Column

The elastic critical load for a column with end conditions other than those of a pin-ended column can be obtained by writing the differential equation describing the equilibrium of a column segment and solving for the constants of integration through enforcement of the boundary conditions.

Figure W8.3.1: Buckling of a pinned-fixed column.

Let us consider the column shown in Fig. W8.3.1*a*, hinged at the base, A, and restrained from rotation at its upper end, B. When buckling occurs, a restraining moment (M_B) at B, and a horizontal reactive force (R) at supports A and B develop (Fig. W8.3.1*b*). The direction and magnitude of these horizontal reactions are determined by noting that they must act to oppose the moment at end B. From this we find that the magnitude of R is M_B/L.

A free body diagram of a segment AD obtained by cutting the column at a distance z from the support A is shown in Fig. W8.3.1*c*. Moment equilibrium of this segment gives

$$\Sigma(M)_D = 0 \quad \rightarrow \quad M = Pu - \frac{M_B}{L} z \tag{W8.3.1}$$

Assuming small deflections, the internal moment is given by:

$$M = -EIu'' \tag{W8.3.2}$$

The equilibrium equation for the column in its buckled shape is therefore given by:

$$EIu'' + Pu = \frac{M_B}{L} z \quad \rightarrow \quad u'' + \alpha^2 u = \frac{M_B}{EI} \frac{z}{L} \tag{W8.3.3}$$

where $\alpha^2 = P/(EI)$ from Eq. W8.1.9. This equation is a linear, nonhomogeneous, second-order differential equation with constant coefficients. The solution of the homogeneous portion is the same as that given in Eq. 8.4.6. The particular solution is given by dividing

the term on that side by α^2. The complete solution is as follows:

$$u = C_1 \sin \alpha z + C_2 \cos \alpha z + \frac{M_B}{P} \frac{z}{L} \tag{W8.3.4}$$

We have four unknowns, namely, the integration constants C_1 and C_2, M_B, and α (or P). The boundary conditions are:

$$\begin{aligned} u &= 0 \text{ at } z = 0 \\ u &= 0 \text{ at } z = L \\ u' &= 0 \text{ at } z = L \end{aligned} \tag{W8.3.5}$$

Using the first two boundary conditions, we get:

$$C_2 = 0; \quad C_1 = -\frac{M_B}{P} \frac{1}{\sin \alpha L} \tag{W8.3.6}$$

Hence,

$$u = \frac{M_B}{P} \left[\frac{z}{L} - \frac{\sin \alpha z}{\sin \alpha L} \right] \tag{W8.3.7}$$

and

$$u' = \frac{M_B}{P} \left[\frac{1}{L} - \alpha \frac{\cos \alpha z}{\sin \alpha L} \right] \tag{W8.3.8}$$

Employing the third boundary condition gives the following :

$$M_B = 0 \tag{W8.3.9}$$

a trivial condition, or

$$\tan \alpha L - \alpha L = 0 \tag{W8.3.10}$$

The smallest nonzero root of this transcendental equation is:

$$\alpha L = 4.493 \tag{W8.3.11}$$

The corresponding buckling load is:

$$P_{cr} = \alpha^2 EI = \frac{20.2EI}{L^2} = \frac{\pi^2 EI}{(0.707L)^2} \approx \frac{2\pi^2 EI}{L^2} = 2P_E \tag{W8.3.12}$$

Thus, the effect of fixing one end of a pin-ended column is to increase its elastic critical load by a factor of 2.

From Eqs 8.4.14 and W8.3.12, we observe that the elastic critical load of a column can be written as:

$$P_{cr} = P_e = \frac{\pi^2 EI}{(KL)^2} \tag{W8.3.13}$$

where L = length of the column

K = effective length factor

KL = effective length of the column

The effect of fixing one end of a pin-ended column is therefore to decrease the effective

length, KL, from L to $0.707L$ and to increase its load carrying capacity by a factor of 2.

W8.4 Inelastic Stability of Axially Loaded Columns

W8.4.1 Reduced and tangent modulus loads

To account for the effects of inelasticity on the stability of ideal, pin-ended columns, two theories were proposed: the reduced modulus theory and the tangent modulus theory. They were originally developed for columns made from materials having a linear elastic stress-strain diagram in the elastic region followed by a continuously nonlinear curve in the inelastic region (see Figs. W8.4.1*d* and W8.4.2*d*).

Figure W8.4.1: Reduced modulus load.

In the ***reduced modulus theory*** (also known as the ***double modulus theory***), the axial load is assumed to remain constant during buckling. That is, no change in load occurs as the column displaces from the straight configuration to the bent one. At buckling, the bending deformation of the column must necessarily cause strain reversal on the convex side of the member (Fig. W8.4.1*b*), with the elastic modulus E governing the stress-strain behavior of those fibers (Fig. W8.4.1*c* and *d*). The concave side of the member, on the other hand, must continue to load inelastically; consequently, the tangent modulus E_t governs the stress-strain behavior of those fibers (Fig. W8.4.1*c* and *d*). The critical load obtained via this model is known as the ***reduced modulus load***, P_r, and is given by [Gerard, 1962; Galambos, 1968]:

$$P_{cr} = P_r = \frac{\pi^2 E_r I}{L^2} = \frac{E_r}{E} P_E \qquad \text{(W8.4.1)}$$

where E_r is known as the reduced modulus. The reduced modulus is a function of the tangent modulus, E_t, the elastic modulus, E, and the geometry of the cross section. For example, for a column with a rectangular cross section, it can be shown [see Gerard, 1962] that:

$$E_r = \frac{4 E E_t}{\left(\sqrt{E} + \sqrt{E_t}\right)} \qquad \text{(W8.4.2)}$$

The reduced modulus load is lower than the Euler load since the ratio E_r/E is always less than unity. The corresponding critical stress is given by:

$$f_{cr} = f_r = \frac{E_r}{E} f_E \qquad \text{(W8.4.3)}$$

Figure W8.4.2: Tangent modulus load.

In the ***tangent modulus theory***, the axial strains are assumed to increase over the entire cross section during buckling (bending). That is, there is a slight increase in the axial load when the inelastic column shifts from the straight (pre-buckling) to the bent (post-buckling) configuration. The amount of load increase is such that strain reversal does not take place during buckling. So, the tangent modulus E_t governs the stress-strain behavior of the entire cross section. As shown in Fig. W8.4.2, E_t is slope of the stress-strain curve at the point of the applied stress at buckling. The associated critical load obtained is known as the ***tangent modulus load***, P_t, and is given by [Gerard, 1962; Galambos, 1968]:

$$P_{cr} = P_t = \frac{\pi^2 E_t I}{L^2} = \frac{E_t}{E} P_E \qquad \text{(W8.4.4)}$$

The tangent modulus load, unlike the reduced modulus load, is independent of the geometry of the cross section. It depends only on material properties. The corresponding critical stress is given by:

$$f_{cr} = f_t = \frac{E_t}{E} f_E \qquad \text{(W8.4.5)}$$

Figure W8.4.3: Inelastic behavior of columns.

To reiterate, the theory underlying the reduced modulus load is based upon the concept that there is no change in load as the column displaces from the straight to the bent configuration. On the other hand, the theory underlying the tangent modulus load requires that an increase in load must accompany the displacement from the straight to the bent configuration. It is therefore not surprising that these two theories produce differing results. The reduced modulus theory predicts buckling loads that are greater than those predicted by the tangent modulus theory. Although most engineers advocated the reduced modulus theory historically, which intuitively had seemed more rational, the scientific consensus reversed once load test results became available and demonstrated closer agreement with the tangent modulus theory.

In 1947, Shanley put forth a theory that clarified the phenomenon of inelastic buckling, and in so doing, resolved the differences between the reduced modulus and the tangent modulus theories. Using a simplified physical model, Shanley [1947] showed that bifurcation will

take place when the axial load reaches the tangent modulus load. After bifurcation, any increase in lateral deflection is accompanied by a slight increase in load. For any finite increase in load above the tangent modulus load, the column assumes equilibrium positions with increasing deflection accompanied by strain reversal on the convex side of the column. Thus, the ***maximum load***, P_{max}, of a perfectly straight column is slightly higher than the tangent modulus load. Also, it was shown that if a column were artificially held in a straight position, as the load was gradually increased to a value somewhere in-between the tangent modulus and reduced modulus loads, and then released, the column would start to bend as it began to take on a slight increase in axial load. However, the magnitude of the increase would be less than that which occurs at the tangent modulus load. Finally, if the column was held in a straight configuration up to the reduced modulus load and then released, it would buckle with no increase in axial load. Thus, we have:

$$P_t < P_{max} < P_r < P_E \qquad \text{(W8.4.6)}$$

Figure W8.4.4: Variation of buckling stress for annealed steel columns.

Unlike the nonlinear stress-strain diagram assumed in the development of the theories mentioned above, mild structural steels have stress-strain curves that feature linearly elastic-perfectly plastic behavior until strain hardening occurs at large strains. By strict application of the tangent modulus concept, the critical stress below F_y is then governed by the Euler formula, and the column curve takes the form shown in Fig. W8.4.4. However, a great variety of carefully performed tests on relatively straight steel columns with carefully

centered axial loads have shown that the column strength predicted by Fig. W8.4.4 is usually higher than the actual strength for hot rolled steel columns of intermediate length. Osgood [1951] attributed this reduction in column strength to the presence of residual (or locked-in) stresses in hot-rolled steel sections. The implication of Osgood's finding is that for structural steel we cannot go directly from a small compressive test specimen to the column strength curve, as in the case of aluminum. However, the research of Osgood [1951] and Yang et al. [1952] made possible the extension of the tangent modulus theory to the analogous critical load theory for steel columns with bilinear stress-strain curves and bisymmetric patterns of residual stress.

Figure W8.4.5: Stub column test.

For hot-rolled steel sections, the part of the member cross section that cools most rapidly is left in residual compression, and the part of the member that cools most slowly is left in residual tension (see Section 2.6.2). Thus, in the case of a wide flange section, the flange tips, possessing relatively more surface area and thus cooling most rapidly, contain residual compressive stresses, whereas the region at the junction between the flange and the web contains residual tensile stresses (Fig. W8.4.5*a*). Maximum compressive residual stresses at the flange tips of rolled sections are typically of the order of 10 to 15 ksi, although values higher than 20 ksi have been measured. The yield stress of the steel has little effect on the magnitude of the residual stress present in rolled shapes.

The presence of residual stresses influences the shape of the average stress vs. average strain curve of the section, as distinct from the curves obtained from coupons cut from the same

member. Consider a short length of a hot-rolled W-shape cut with its ends carefully machined, and placed between the plates of a testing machine. If it is compressed gradually in a concentric test, called a ***stub column test***, the end faces will remain parallel, as no bending occurs (Fig. W8.4.5*a*). The length of the stub column decreases as the compression force is increased. This change, Δ, divided by the original length of the stub column, *s*, represents the unit strain ϵ^* caused by the applied average stress, $f^* = P/A$. Figure W8.4.5*c* shows the type of curve obtained in this manner [Galambos, 1998]. If a compressive residual strain of magnitude ϵ_{rc} were present at the flange tips, then yielding would commence when the applied strain ϵ^* equals $(\epsilon_y - \epsilon_{rc}) = \epsilon^*_{pl}$. The corresponding average stress f^*_{pl} is known as the ***reduced proportional limit.*** When a stub column is strained above the reduced proportional limit, portions of the cross section yield. If the yielded parts are perfectly plastic, the axial stiffness of those zones reduces to zero. The overall stress-strain relationship for a stub column would therefore be nonlinear. With sufficient straining, the average stress would eventually reach the yield stress and the load corresponds to the squash load the cross section, P_y, given by:

$$P_y = A F_y \qquad \text{(W8.4.7)}$$

Thus, the influence of residual stresses in columns is to make the yielding over the cross section a gradual process and to make the stress-strain relationship nonlinear above the reduced proportional limit, as shown in Fig. W8.4.5*c*. The slope of the stub column stress-strain curve is the tangent modulus E_t^* of the member. Also shown in the figure is the stress-strain curve for a coupon. Unlike a stub column, a coupon, is free of residual stress. Therefore, its stress-strain relationship exhibits elastic-perfectly plastic behavior.

Figure W8.4.6: Variation of buckling stress for straight, pin-ended, rolled steel columns.

There are two general methods by which the strength of pin-ended hot-rolled steel columns loaded into the plastic domain can be obtained:

- The first method is experimental in that, to start with, an average stress-average strain diagram is determined from a stub column test. Column strength can then be determined using the tangent modulus E_t^* of the average stress-average strain diagram along with the proper slenderness ratio for strong or weak axis bending (Fig. W8.4.6).

$$P_{cr} = P_t^* = \frac{\pi^2 E_t^* I}{L^2} \tag{W8.4.8}$$

$$f_{cr} = f_t^* = \frac{\pi^2 E_t^*}{(L/r)^2} = \frac{E_t^*}{E} f_E \tag{W8.4.9}$$

Figure W8.4.6 shows a typical tangent modulus column curve f_t^* vs. (L/r). Due to the effects of residual stress, the tangent modulus column curve falls below the yield plateau and the Euler hyperbola in the short and intermediate slenderness ranges.

- The second approach to the problem is an analytical solution [Huber and Beedle, 1954]. It makes use of the residual stress distribution, either measured or assumed, along with the stress-strain (f - ϵ) diagram for the material as obtained from a coupon test. When a column is strained above the reduced proportional limit, portions of the cross section yield. As the yielded parts are perfectly plastic, the bending stiffness of those zones reduces to zero. The theoretical buckling strength will be equal to that

of a new column having a moment of inertia equal to the moment of inertia of the remaining elastic portion of the cross section.

$$P_{cr} = P_H = \frac{\pi^2 E I_e}{L^2} \tag{W8.4.10}$$

$$f_{cr} = f_H = \frac{\pi^2 E\left(I_e/I\right)}{(L/r)^2} = \frac{I_e}{I} f_E \tag{W8.4.11}$$

The above equations are the basic equations for determining the inelastic strength of a straight, pin-ended steel column containing residual stresses [Huber and Beedle, 1954]. Based on the methods described above, column strength curves have been developed for weak and strong axis buckling with various distributions of residual stress. The results show that the residual stresses are of particular importance for columns with slenderness ratios varying from 50 to 120, a range that includes a large percentage of practical columns. As previously mentioned, residual stresses in rolled shapes tend to be independent of the yield stress. Thus, reductions in axial strength tend to be smaller for rolled shapes of higher strength steels. The results also show that for the same slenderness ratio, I-shaped column sections bent about the weak axis carry less load than columns bent about the strong axis. Since 1961, structural steel design based on the AISC Allowable Stress Design Specification has used column curves developed by applying the experimental tangent modulus method described above.

The limiting slenderness ratio for columns of intermediate length is generally defined as the boundary between elastic and inelastic buckling. That boundary is dependent on the level of the maximum residual compressive stress, f_{rc} (or the residual proportional limit, f_{pl}^*). We

have:

$$F_y = \frac{\pi^2 E}{(KL/r)_o^2}; \qquad f_{pl}^* = (F_y - f_{rc}) = \frac{\pi^2 E}{(KL/r)_{pl}^2} \tag{W8.4.12}$$

$$\lambda_{pl} = \frac{(KL/r)_{pl}}{(KL/r)_o} = \sqrt{\frac{F_y}{(F_y - f_{rc})}} = \frac{1}{\sqrt{1 - (f_{rc}/F_y)}} \tag{W8.4.13}$$

For $f_{rc} = 0.5F_y$, we obtain: $\lambda_{pl} = \sqrt{2} = 1.414$.

W8.4.2 Maximum Strength

The concept of a constant tangent modulus for a particular axial load is only applicable to perfectly straight columns and is therefore an unsatisfactory means of dealing with real members having geometric imperfections and load eccentricities. The maximum strength of a nominally straight, nominally axially loaded, pin-ended, hot-rolled steel column may, in principle, be expressed by the function, F:

$$P_{ult} = F(L, f_g, f_y, f_r, f_i, f_e) \tag{W8.4.14}$$

where L = length of the column

f_g = function representing the geometry of the cross section (dimensions b_f, t_f, d and t_w for a W-shape, for example)

f_y = function representing the yield stress distribution in the cross section

f_r = function representing the residual stress distribution in the cross section

f_i = function representing the initial geometry of the unloaded column

f_e = function representing the end eccentricity of the axial load

These parameters can be divided into two groups. The first group, f_g, f_y, and f_r, influences the internal flexural resistance. The second group, f_i and f_e, affects the external moment at a section.

The European Convention for Constructional Steelwork (ECCS) recommends the use of multiple column curves to determine the strength of columns. These curves are based on:

- A very extensive program of experimental research into the mechanical properties of steel and the buckling strength of columns of various cross sections and slenderness ratios. The test program has included well over 1000 column tests [ECCS, 1972; ECCS, 1977; Sfintesco, 1970; Beer and Schulz, 1970]. The columns were taken at random from various stockyards of steel fabricators in several European countries in an effort to furnish representative samples of columns normally used in actual structures. They were tested under conditions very close to those found in actual structures, and in sufficient number to obtain mean ultimate loads and standard deviations possessing statistical validity.
- An equally comprehensive program of theoretical research using computer models to study the inelastic behavior of columns with and without geometrical or structural imperfections.

The criteria adopted by ECCS is that the nominal failure load for a series of specimens is the mean measured value minus two standard deviations. Thus, assuming that the data is normally distributed, there is a 97.7 percent probability that the nominal failure load will be below the member's actual strength and a 2.3 percent probability that it will be above.

Major research conducted by Bjorhovde [1972] at Lehigh University examined the deterministic and probabilistic characteristics of column strength in general and developed an extensive database for the maximum strength of centrally loaded compression members. The shapes studied encompassed the major shapes used for columns, including rolled and welded shapes for which measured residual-stress distributions were available.

The maximum strength of these columns was determined assuming that the initial crookedness was of sinusoidal shape having a maximum amplitude of 1/1000 of the column length, and that the end restraint was zero. Column curves were then developed using the ***column-slenderness parameter***, $\lambda_c = (KL/r\pi)\sqrt{F_y/E}$. The value $\lambda_c = 1$ corresponds to the value of KL/r for which the elastic flexural buckling stress is equal to the yield stress. The set of 112 column curves thus obtained represent essentially the whole spectrum of steel column behavior. After a detailed study of these results, the sections were divided into three groups. The first group included 30 curves, and the second and the third groups, 70 and 12 curves, respectively. The resulting three curves for these subgroups are known as ***SSRC column strength curves 1, 2, and 3*** (Fig. 8.6.2). Bjorhovde [1972] also developed multiple column curves where the initialout-of-straightness was equal to its mean value of 1/1470 of the column length. Those curves are known as ***SSRC column strength curves 1P, 2P, and 3P***. The single column curve that is used in Chapter E of the LRFD specification for design of columns (discussed in Section 8.10.1) is identical to SSRC 2P [Galambos, 1998; Tide, 1985].

W8.5 Elastic Buckling of a Uniformly Compressed Rectangular Plate with Simply Supported Edges

The stability of a rectangular plate that is simply supported on all four edges and subjected to uniform compressive forces in one direction will be considered (Fig. W8.5.1). We will assume:

1. The plate is originally perfectly flat.
2. The plate is made of a linearly elastic, homogeneous material.
3. The compressive loads are applied along the plane of the middle surface of the plate.
4. Deflections considered are small; the significant deflection at buckling is of the order of the thickness of the plate or less.

Figure W8.5.1: Rectangular plate with simply supported edges under uniform compression in x-direction.

The equilibrium equation for a buckled plate is given by a fourth-order, homogeneous, partial differential equation [Bleich, 1952; Timoshenko and Gere, 1961; Gerard, 1962; Chajes, 1974]:

$$\frac{Et^3}{12(1-\mu^2)}\left[\frac{\partial^4 w}{\partial x^4} + 2\frac{\partial^4 w}{\partial x^2 \partial y^2} + \frac{\partial^4 w}{\partial y^4}\right] + N_x \frac{\partial^2 w}{\partial x^2} = 0 \qquad \text{(W8.5.1)}$$

with

$$N_x = t f_x \qquad \text{(W8.5.2)}$$

where E = modulus of elasticity

μ = Poisson's ratio

t = thickness of the plate

w = deflection of the plate normal to its original orientation

N_x = load per unit width of plate

f_x = uniform compressive stress in the x direction

A solution to Eq. W8.5.1 is obtained when the deflection, w, and the compressive load, N_x, are found such that the equation is satisfied both at the boundaries and also over the entire surface of the plate. One solution is to assume the deflection w to be given by a series, each term of which initially and automatically satisfies the boundary conditions. The task, then, is to determine the coefficients of the terms in the series and the loading, N_x, that satisfy the differential equation at every point on the surface of the plate. A convenient series for the simply supported plate under consideration is the double sine series:

$$w = \sum_{m=1}^{\infty} \sum_{n=1}^{\infty} A_{mn} \sin\frac{m\pi x}{a} \sin\frac{n\pi y}{b} \qquad \text{(W8.5.3)}$$

where m and n are the number of half sine waves in the x and y directions, respectively; A_{mn} is the unknown coefficient for each m-n pair; and a and b are the length and width of the plate, respectively. The above series satisfies the boundary conditions for deflections because for $x = 0$ and $x = a$, as well as for $y = 0$ and $y = b$, the computed edge deflection equals zero.

Edge moments for a rectangular plate are given by [Chajes, 1974; Gerard, 1962]:

$$M_x = -D\left[\frac{\partial^2 w}{\partial x^2} + \mu\frac{\partial^2 w}{\partial y^2}\right]; \quad M_y = -D\left[\frac{\partial^2 w}{\partial y^2} + \mu\frac{\partial^2 w}{\partial x^2}\right] \tag{W8.5.4}$$

$$D = \frac{Et^3}{12(1-\mu^2)} \tag{W8.5.5}$$

where M_x and M_y are bending moments per unit width of plate and D is the flexural rigidity per unit width of plate. From Eq. W8.5.3, $\frac{\partial^2 w}{\partial x^2} = 0$ and $\frac{\partial^2 w}{\partial y^2} = 0$ at the four edges. So, Eq. W8.5.3 also satisfies the simple support boundary conditions that the edge moments equal zero. By substituting $f_x t$ for N_x and the appropriate derivatives of Eq. W8.5.3 into Eq. W8.5.2, we obtain:

(W8.5.6)

$$\sum_{m=1}^{\infty}\sum_{n=1}^{\infty} A_{mn}\left[\pi^4\left(\frac{m^2}{a^2}+\frac{n^2}{b^2}\right)^2 - \frac{tf_x}{D}\frac{m^2\pi^2}{a^2}\right]\sin\frac{m\pi x}{a}\sin\frac{n\pi y}{b} = 0$$

The left hand side of this equation consists of a sum of an infinite number of independent functions. The only way such a sum can vanish is if the coefficient of every one of the terms is equal to zero. Thus:

$$A_{mn}\left[\pi^4\left(\frac{m^2}{a^2}+\frac{n^2}{b^2}\right)^2 - \frac{tf_x}{D}\frac{m^2\pi^2}{a^2}\right] = 0 \tag{W8.5.7}$$

This relation can be satisfied in one of two ways: either $A_{mn} = 0$ or the term in the brackets equals zero. If $A_{mn} = 0$, f_x can have any value. This is a trivial solution indicating that the plate remains in equilibrium at all loads, provided that the plate remains perfectly straight. The nontrivial solution that leads to the critical load is obtained by setting the expression in the brackets equal to zero. Thus,

(W8.5.8)

$$f_{cr\,m,n} = f_x = \frac{\pi^2 E t^2}{12(1-\mu^2)}\frac{a^2}{m^2}\left(\frac{m^2}{a^2}+\frac{n^2}{b^2}\right)^2 \qquad \begin{matrix} m = 1,2,3,... \\ n = 1,2,3,... \end{matrix}$$

According to Eq. W8.5.8, f_{cr} is a function of the dimensions and the physical properties of the plate, and the number of half-waves into which the plate buckles (m and n). Since we are interested in the lowest critical load, the values of m and n that minimize Eq. W8.5.8 must be determined. It is evident that f_{cr} increases as n increases and that $n = 1$, therefore, results in a minimum value for f_{cr}. Thus, the plate buckles in a single half-wave in the y-direction. Consequently, the critical compressive stress is:

$$f_{cr} = f_{cr\,m,1} = \frac{\pi^2 E}{12(1-\mu^2)}\frac{k_c}{(b/t)^2} \tag{W8.5.9}$$

where

$$k_c = \left(\frac{mb}{a}+\frac{a}{mb}\right)^2 \tag{W8.5.10}$$

The term k_c is generally referred to as the ***buckling coefficient***. It depends upon the ratio a/b, called the ***aspect ratio*** of the plate, and the parameter m, an integer, which denotes the number of half-waves into which the plate buckles longitudinally. The smallest value of f_{cr} corresponds to the smallest value of k_c and is obtained by minimizing Eq. W8.5.10 with respect to m. Thus,

(W8.5.11)

$$\frac{\partial}{\partial m}\left[m\frac{b}{a}+\frac{a}{bm}\right]^2 = 2\left[\frac{mb}{a}+\frac{a}{bm}\right]\left[\frac{b}{a}-\frac{a}{bm^2}\right] = 0 \rightarrow m = \frac{a}{b}$$

Substituting into Eq. W8.5.10 results in:

$$k_{c\,\min} = 4 \tag{W8.5.12}$$

Equation W8.5.9 then becomes

$$f_{cr} = \frac{\pi^2 E}{12(1 - \mu^2)} \frac{4}{(b/t)^2} \qquad \text{(W8.5.13)}$$

Since a simply supported plate must buckle into a whole number of half-waves, to satisfy edge conditions, the aspect ratio *a/b*, which according to Eq. 8.2.11 is equal to *m*, must be an integer. The critical stress given by Eq. W8.5.13 is thus valid only when *a/b* is a whole number. For plates that fall into this category, the buckling pattern consists of a single half-wave in the *y*-direction and *a/b* half-waves in the *x*-direction. In other words, the plate buckles into *a/b* half waves, each having a length equal to its width (thus dividing the plate into *a/b* squares), as shown in Fig. W8.5.2.

Figure W8.5.2: Buckling of a long thin rectangular plate under edge compression.

Figure W8.5.3: Buckling coefficients for a simply supported, rectangular flat plate under edge compression.

Figure W8.5.3 shows the variation of k_c with *a/b* for different values of *m*. Setting $m = 1$ in Eq. 8.2.10, the variation of k_c with *a/b* given by the curve labeled $m = 1$ is obtained. In a similar manner, by letting *m* in Eq. W8.5.10 take on successively higher values, the curves for $m = 2, 3, 4$ are obtained. Because values of *m* vary from one to infinity, it is seen that there exists an unlimited number of values for k_c corresponding to any given *a/b*. We are interested in only the smallest value – the value that results in the smallest critical stress at which a given plate buckles. The solid line in Fig. W8.5.3, obtained by connecting the lower

branch of the various curves gives the critical value of k_c as a function of a/b. In addition, for any noninteger value of a/b, the solid line indicates the number of half-waves that will form in the longitudinal direction. Thus, between aspect ratios of 1 and 2, k_c rises along the $m = 1$ curve, and the buckled form of the plate is that of one half-wave until the intersection with $m = 2$. Beyond the intersection, the plate buckles into two half-waves, and k_c decreases to the minimum value of 4 and later rises until the intersection with $m = 3$. At that point another half-wave appears in the buckled form in the longitudinal direction, and the process is repeated. From Fig. W8.5.3 we observe that the transition from m to $m + 1$ half sine waves occurs at the point at which the two corresponding curves have equal ordinates; that is:

(W8.5.14)

$$\frac{m}{\alpha} + \frac{\alpha}{m} = \frac{(m+1)}{\alpha} + \frac{\alpha}{(m+1)} \quad \rightarrow \quad \alpha = \sqrt{m(m+1)}$$

where $\alpha = a/b$. For a long plate,

$$\alpha = \sqrt{m(m+1)} \approx m \tag{W8.5.15}$$

or

$$\xi = \frac{a}{m} \approx b \tag{W8.5.16}$$

where ξ is the length of the half sine wave. Eqs. W8.5.14 and W8.5.15 indicate that the number of half-waves increases with the aspect ratio. For a long plate, we see from Eq. W8.5.6 that the length of the longitudinal half sine wave equals approximately the width of the plate, and therefore the buckled plate is partitioned into squares as mentioned earlier.

In steel structures, the behavior of long plates having relatively large aspect ratios is of great

interest, because such plates are representative of the individual elements that comprise the cross sections of rolled and built-up column shapes. As seen from Fig. W8.5.3, whenever a/b exceeds 4, a value of $k_c = 4$ can be assumed for determining the critical buckling stress of a plate simply supported along four edges and subjected to uniform compressive stress in the longitudinal direction. That is:

$$f_{cr} = \frac{4\pi^2 E}{12(1 - \mu^2)(b/t)^2} \qquad for \quad \frac{a}{b} \geq 4 \qquad \text{(W8.5.17)}$$

The compressive buckling stress of flat plates with various types of boundary conditions can be represented in the following format:

$$f_{cr} = \frac{\pi^2 E}{12(1 - \mu^2)} \frac{k_c}{(b/t)^2} \qquad \text{(W8.5.18)}$$

where E = modulus of elasticity

μ = Poisson's ratio

t = thickness of the plate

b = width of the plate

k_c = plate buckling coefficient

References

W8.1 Beer, H. and Schulz, G. [1970]: "Bases Théoriques des Courbes Européennes de Flambement (Theoretical Basis for the European Column Curves)," *Construction Métallique,* Paris, no.3, September, p. 58.

W8.2 Bjorhovde, R. [1972]: "Deterministic and Probabilistic Approaches to the Strength

of Steel Columns," Ph.D. Dissertation, Lehigh University, Bethlehem, PA, May.

W8.3 Bleich, F. [1952]: *Buckling Strength of Metal Structures,* Engineering Societies Monographs, McGraw-Hill, New York, NY.

W8.4 Chajes, A. [1974]: *Principles of Structural Stability Theory,* Waveland Press Inc., Prospect Heights, IL.

W8.5 Considere, A. [1891]: "Resistance des pieces comprimees ," *Congres international de procedes de construction*, Paris, vol. 3, p. 371.

W8.6 ECCS [1972]: *1st International Colloquium on Stability,* European Convention for Constructional Steelworks, Paris.

W8.7 ECCS [1977]: *2nd International Colloquium on Stability,* Introductory Report, Liége, European Convention for Constructional Steelworks.

W8.8 Engesser, F. [1889]: "Uber die Knickfestigkeit geraderstaben," *Zeitschrift fur Architektur und Ingenierurwesen,* vol. 35, p. 455.

W8.9 Engesser, F. [1895]: "Zeitschrift fur Architektur und Ingenieurwesen," *Schweizerische Bauzeitung,* vol. 26, p. 24.

W8.10 Euler, L. [1744]: "De curvis elasticis," Lausanne and Geneva. The Euler formula was derived in a later paper, "Sur la force de colonnes," published 1759 in the Memoires de l'Academie de Berlin.

W8.11 Galambos, T. V. [1968]: *Structural Members and Frames,* Prentice-Hall, Englewood Cliffs, NJ.

W8.12 Galambos, T. V., ed.[1998]: *Guide to Design Criteria for Metal Compression Members,* 5th ed., Structural Stability Research Council, John Wiley & Sons, New York, NY.

W8.13 Gerard, G. [1962]: *Introduction to Structural Stability Theory,* McGraw-Hill Book

Co., New York, NY.

W8.14 Huber, A. W., and Beedle, L. S. [1954]: "Residual Stress and the Compressive Strength of Steel," *Welding Journal,* vol. 33, December, p. 5598.

W8.15 Osgood, W. R. [1951]: "The Effect of Residual Stress on Column Strength," Proceedings First U.S. National Congress of Applied Mechanics, June, p. 415.

W8.16 Sfintesco, D., ed. [1976]: *Manual of the Stability of Steel Structures,* 2nd ed., European Convention for Constructional Steel Works, ECCS, Paris.

W8.17 Shanley, F. R. [1947]: "Inelastic Column Theory," *Journal of Aeronautical Sciences,* vol. 14, no. 5, pp. 261– 267, May.

W8.18 Tide, R. [1985]: "Reasonable Column Design Equations," Proceedings 1985 Annual Technical Session, Cleveland, OH, Structural Stability Research Council, Lehigh University, Bethlehem, PA.

W8.19 Timoshenko, S. P. and Gere, J. M. [1961]: *Theory of Elastic Stability,* McGraw-Hill Book Company, New York, NY.

W8.20 Yang, H., Beedle, L. S. and Johnston, B. G. [1952]: "Residual Stress and the Yield Strength of Steel Beams," *Welding Journal Research Supplement,* vol. 31, pp. 224–225.

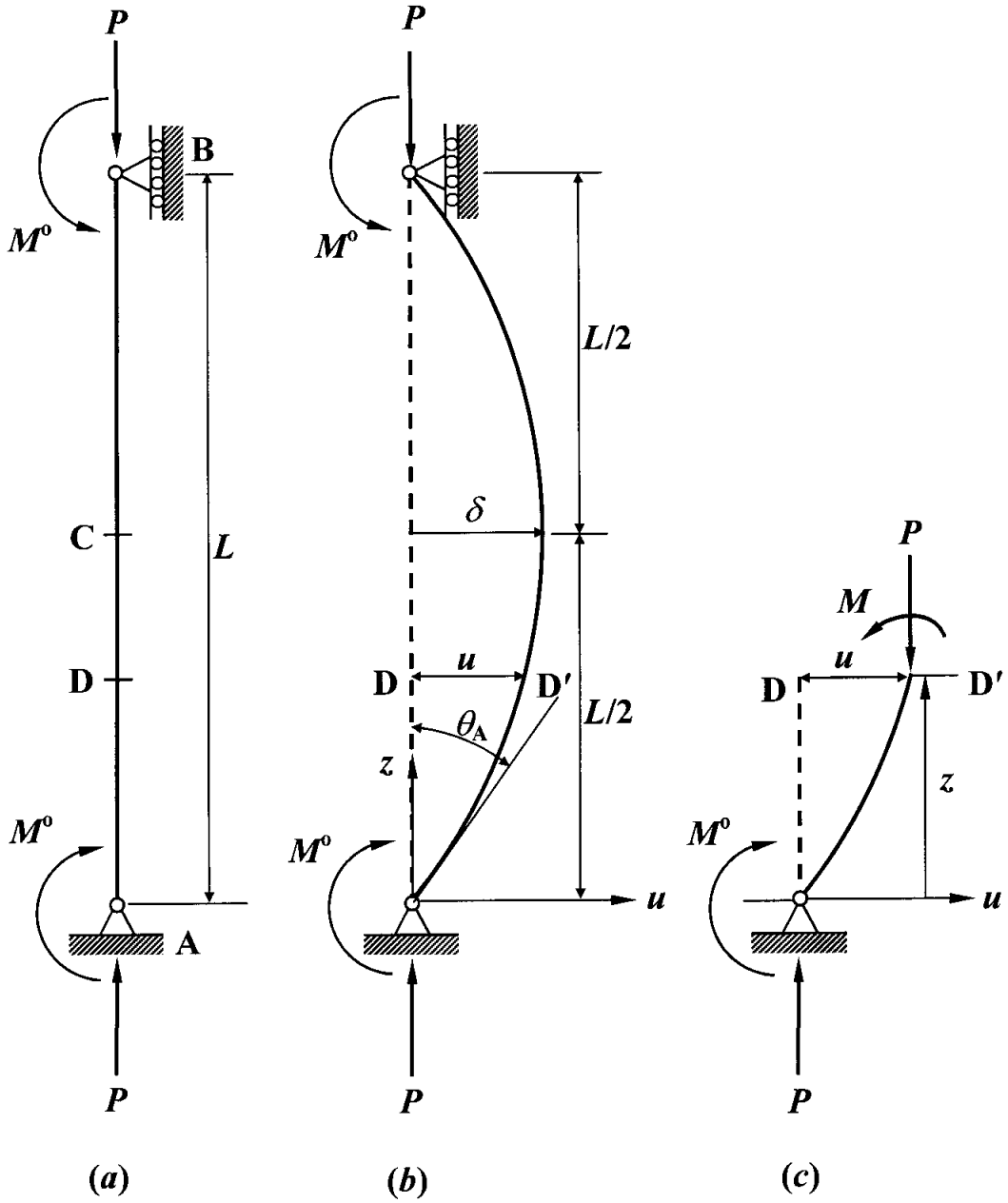

Figure W8.1.1: Model for evaluating rotational stiffness of a column.

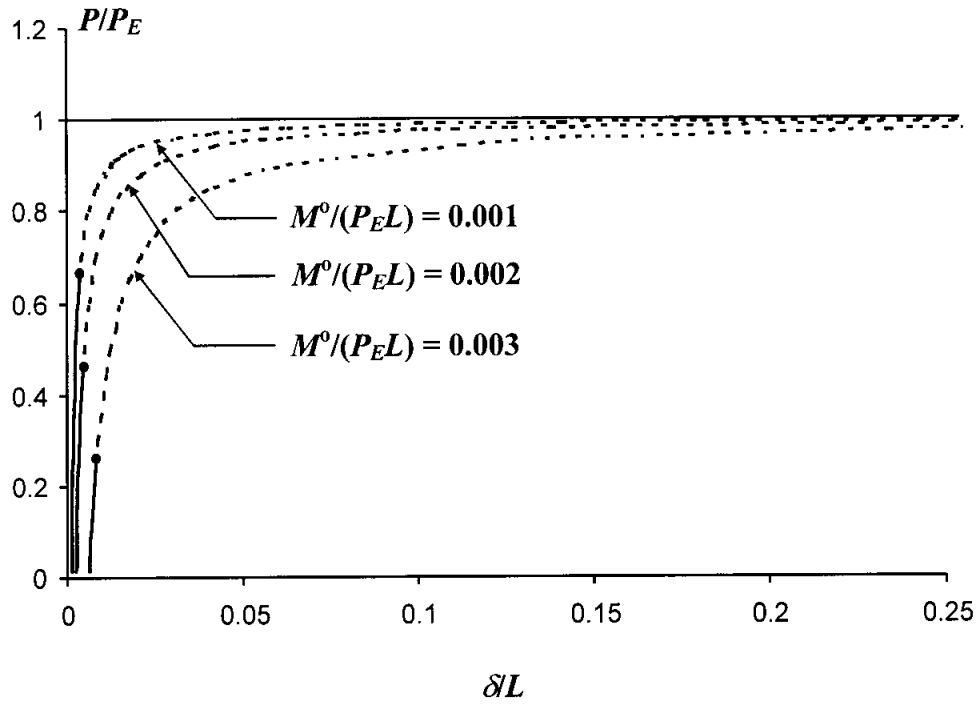

Figure W8.1.2: Variation of deflection with axial load for a pin-ended column with end moments.

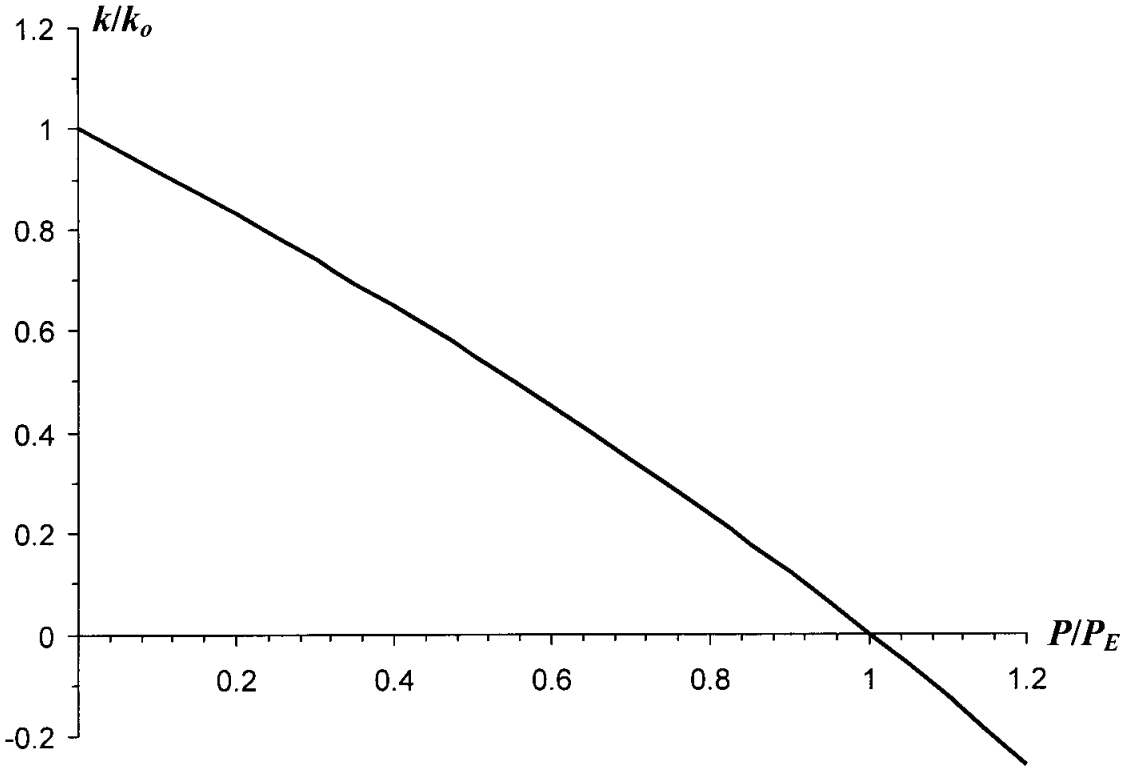

Figure W8.1.3: Variation of rotational stiffness with axial load for a pin-ended column.

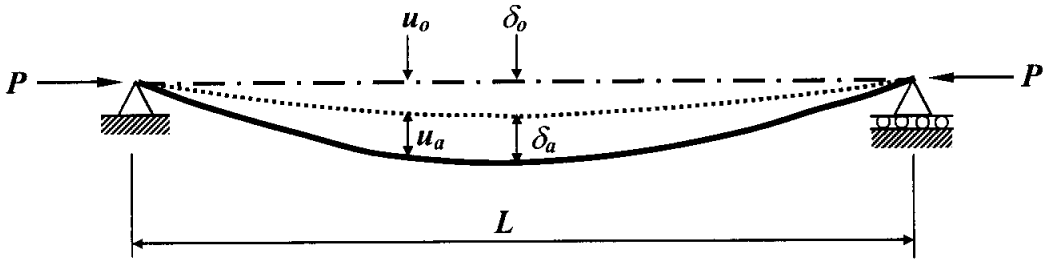

Figure W8.2.1: Imperfect pin-ended column.

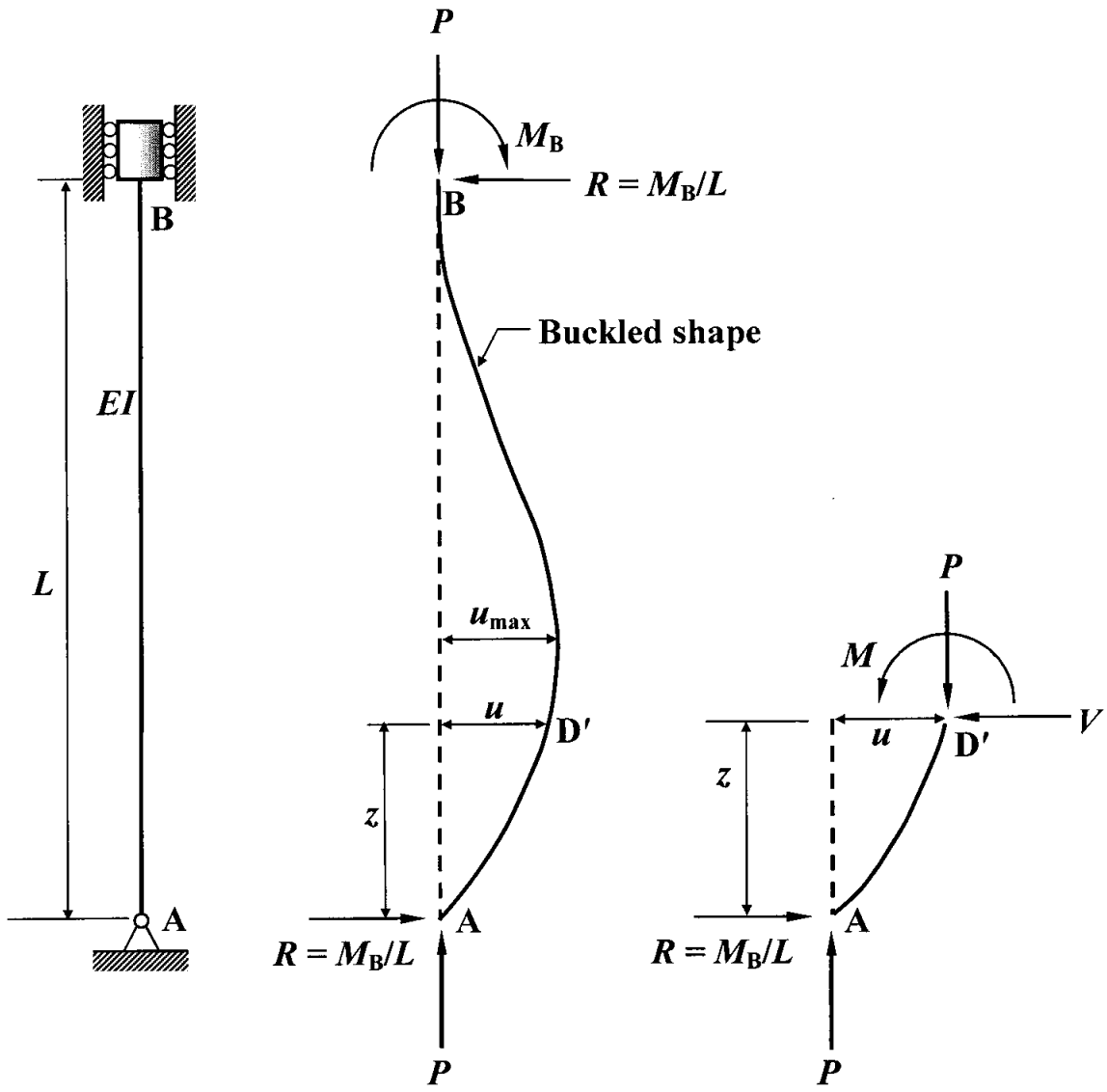

Figure W8.3.1: Buckling of a pinned-fixed column.

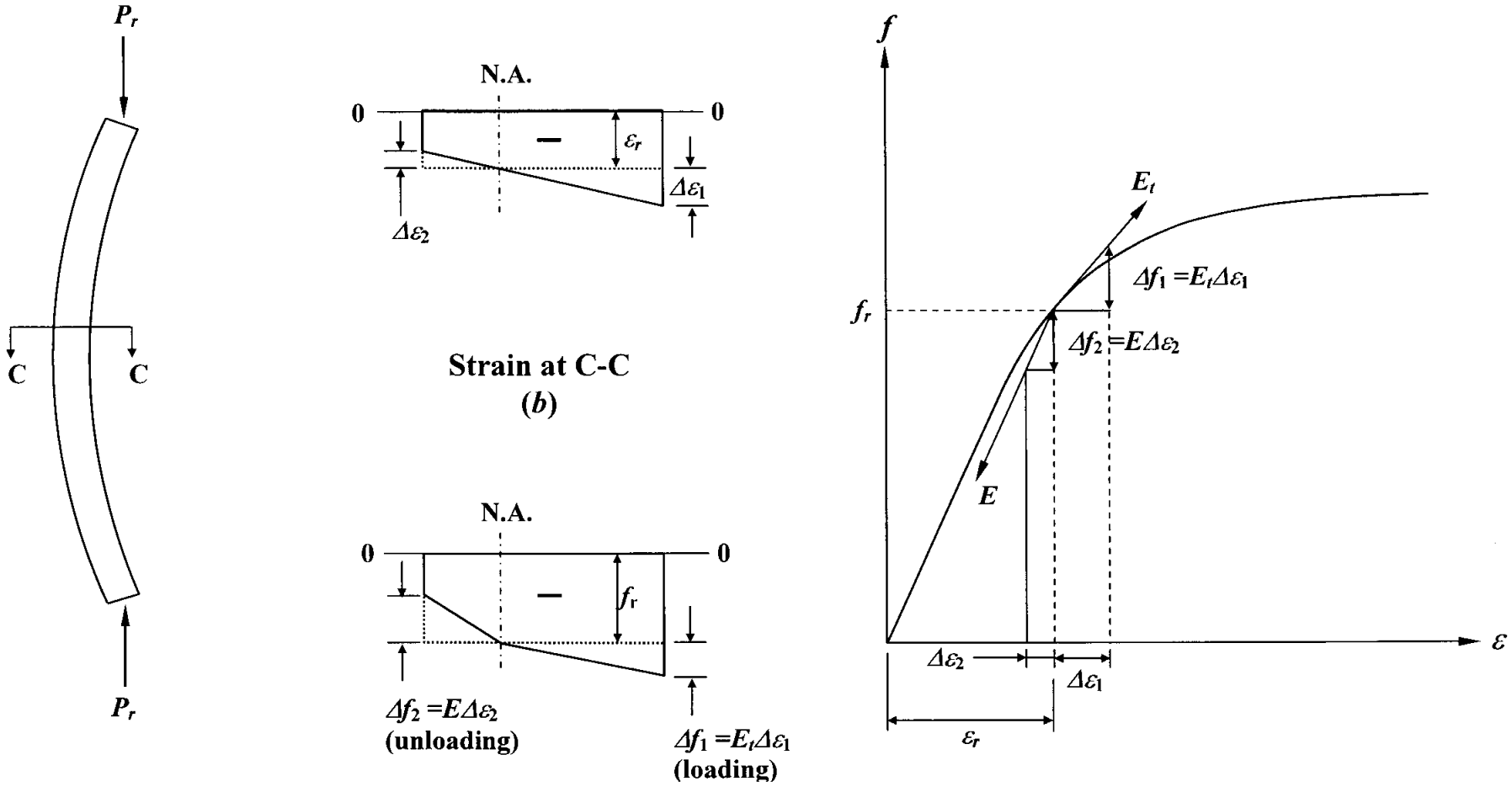

Figure W8.4.1: Reduced modulus load.

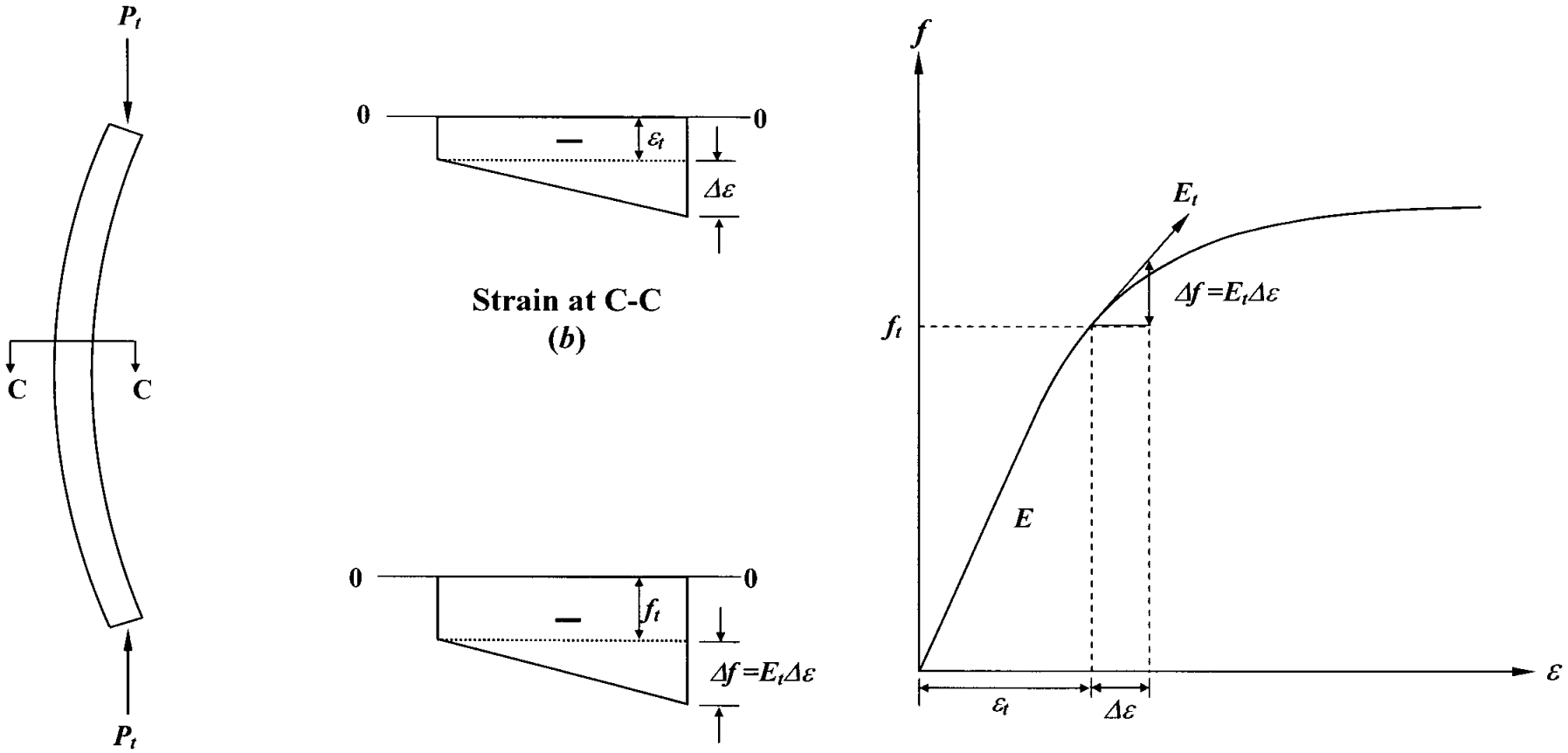

Figure W8.4.2: Tangent modulus load.

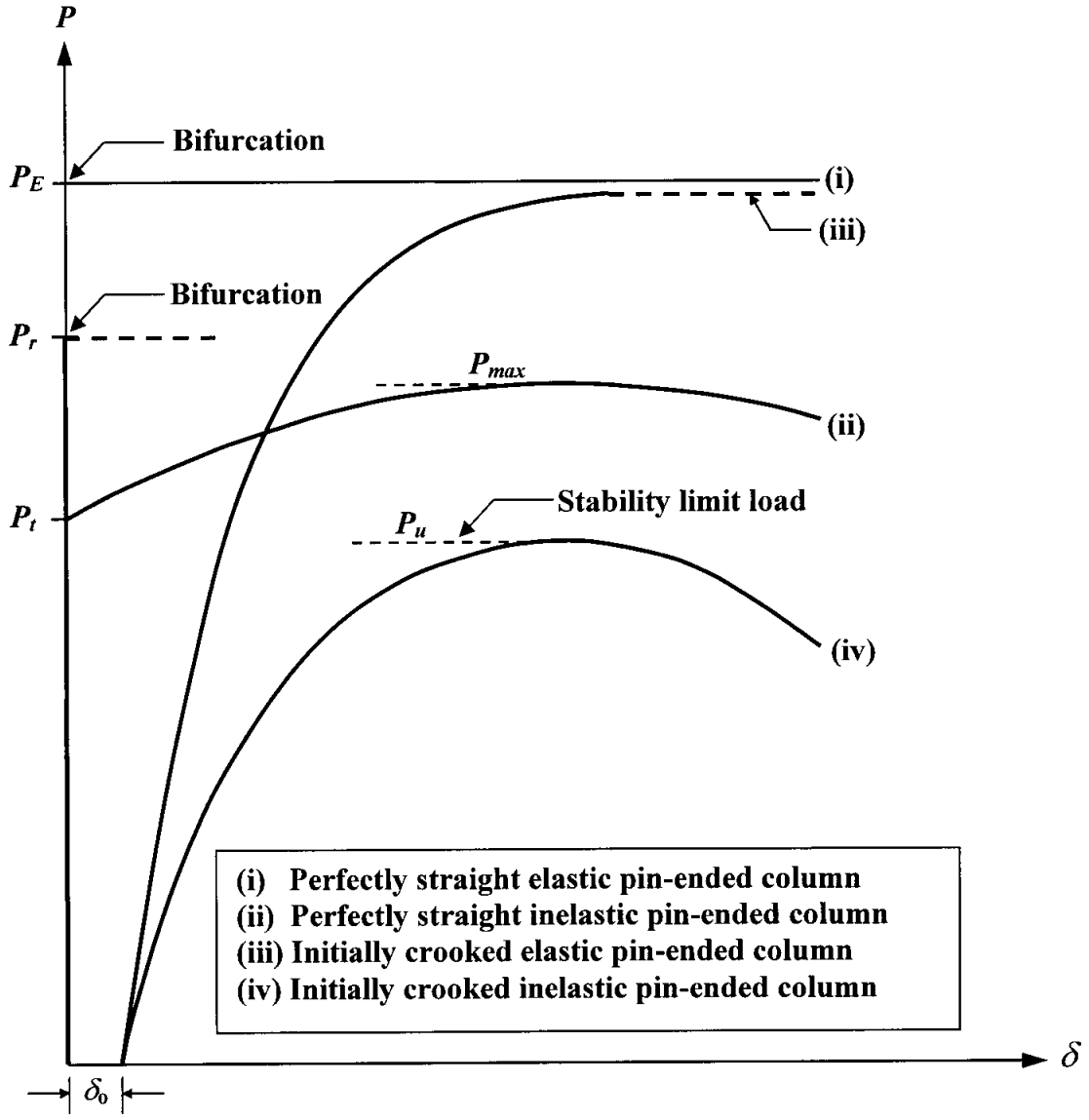

Figure W8.4.3 Inelastic behavior of columns.

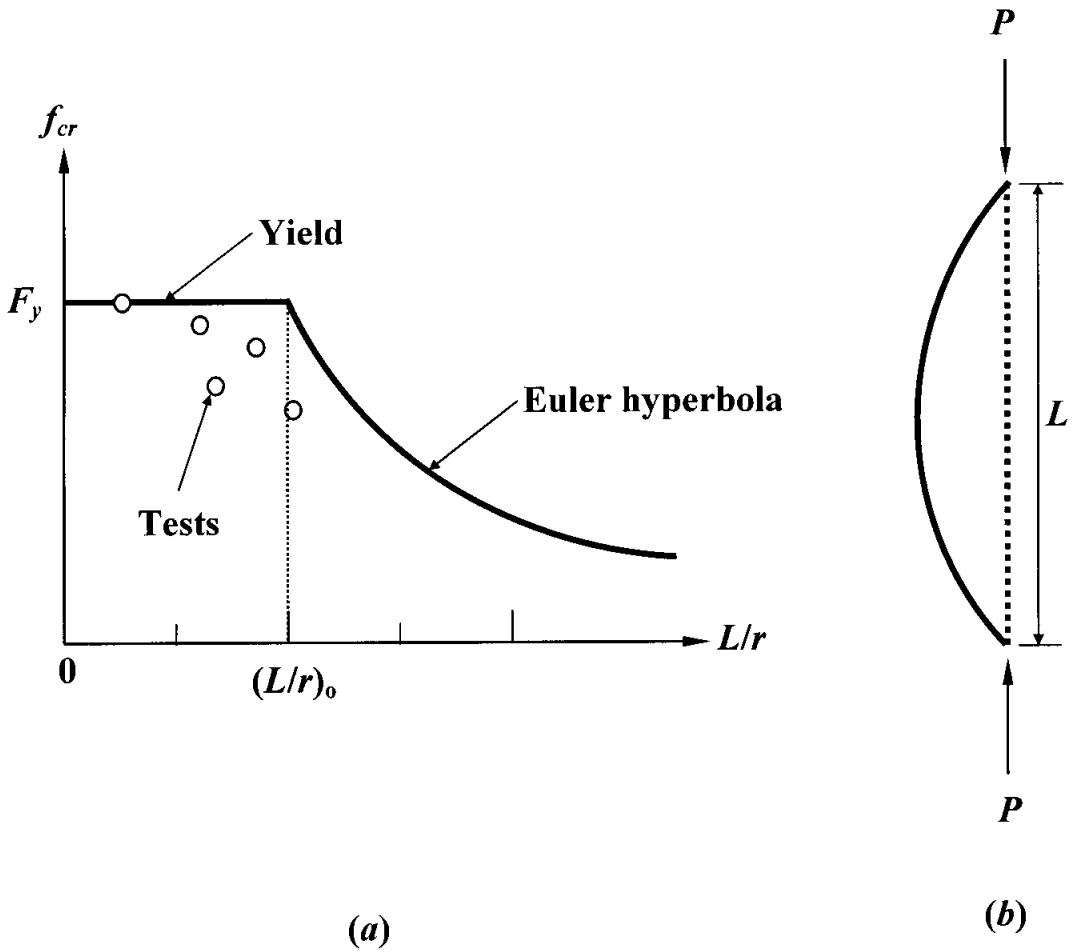

Figure W8.4.4: Variation of buckling stress for annealed steel columns.

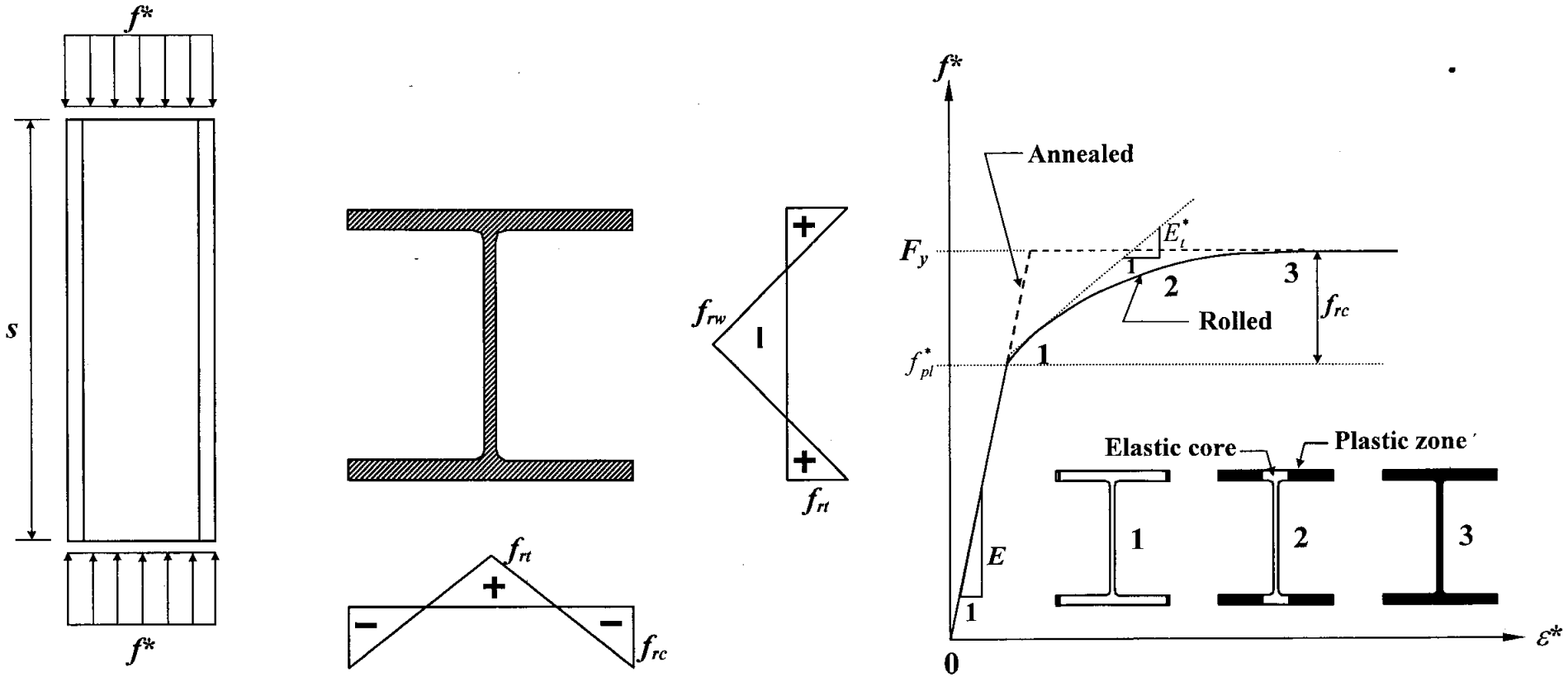

Stub column
(*a*)

Residual stresses
(*b*)

Average stress - average strain diagram
(*c*)

Figure W8.4.5: Stub column test.

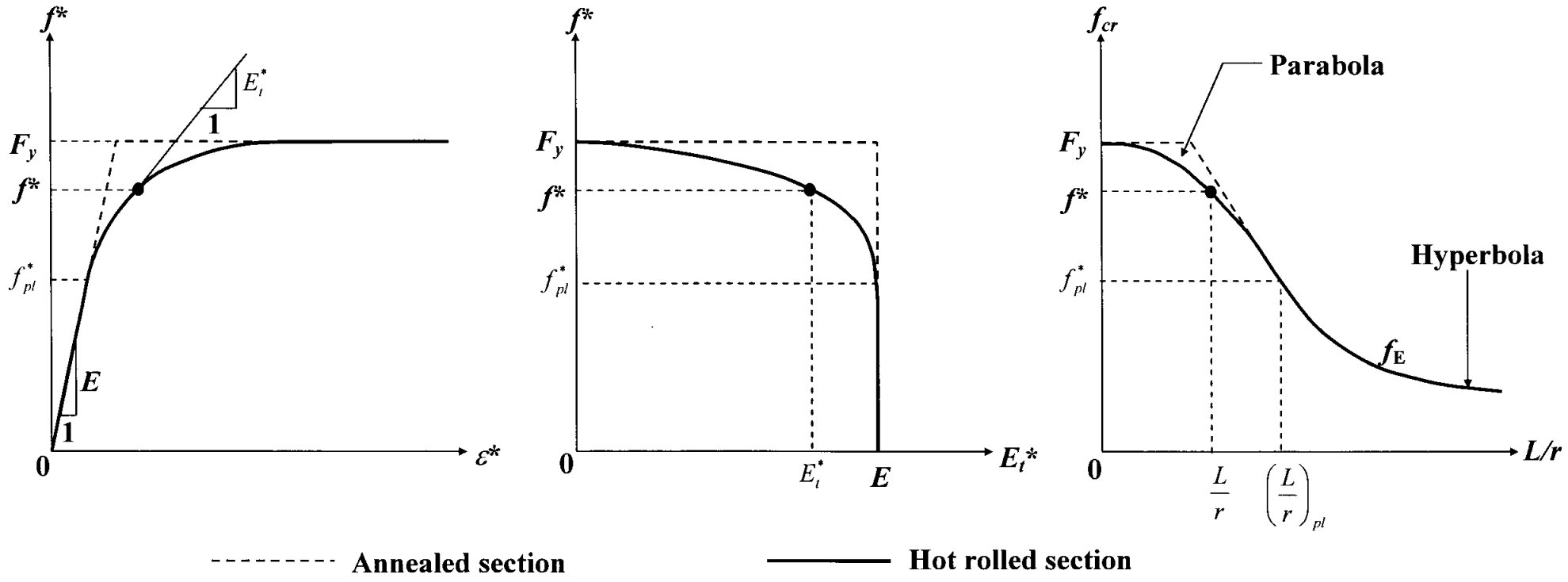

Figure W8.4.6: Variation of buckling stress for straight, pin-ended, rolled steel columns.

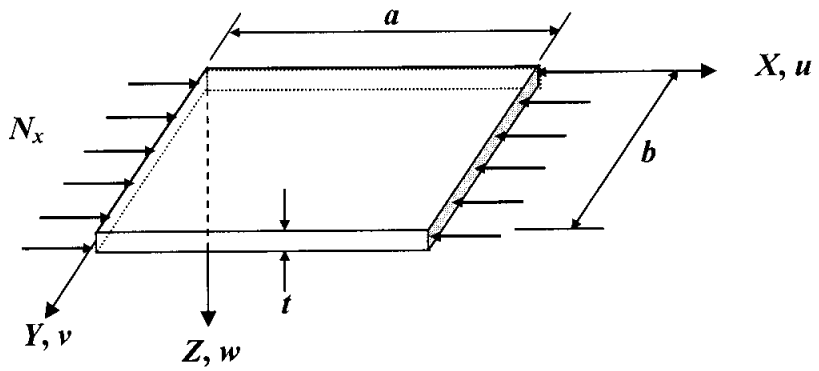

(*a*)

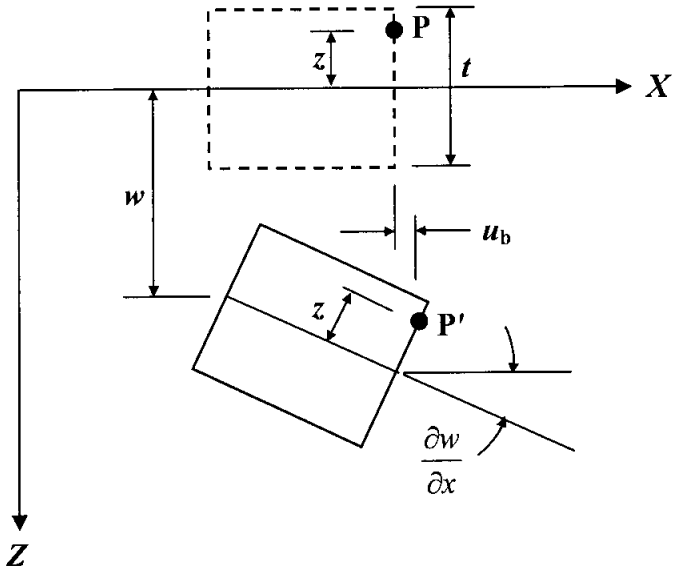

Displacements in *x*-*z* plane

(*b*)

Figure W8.5.1: Rectangular plate with simply supported edges under uniform compression in *x*-direction.

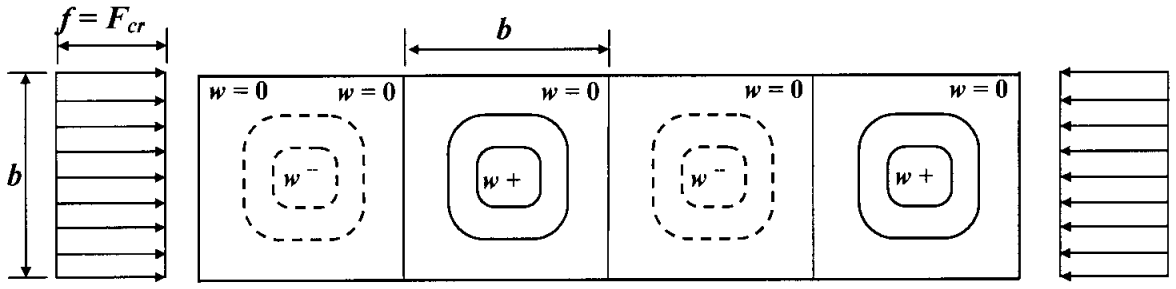

(*a*)

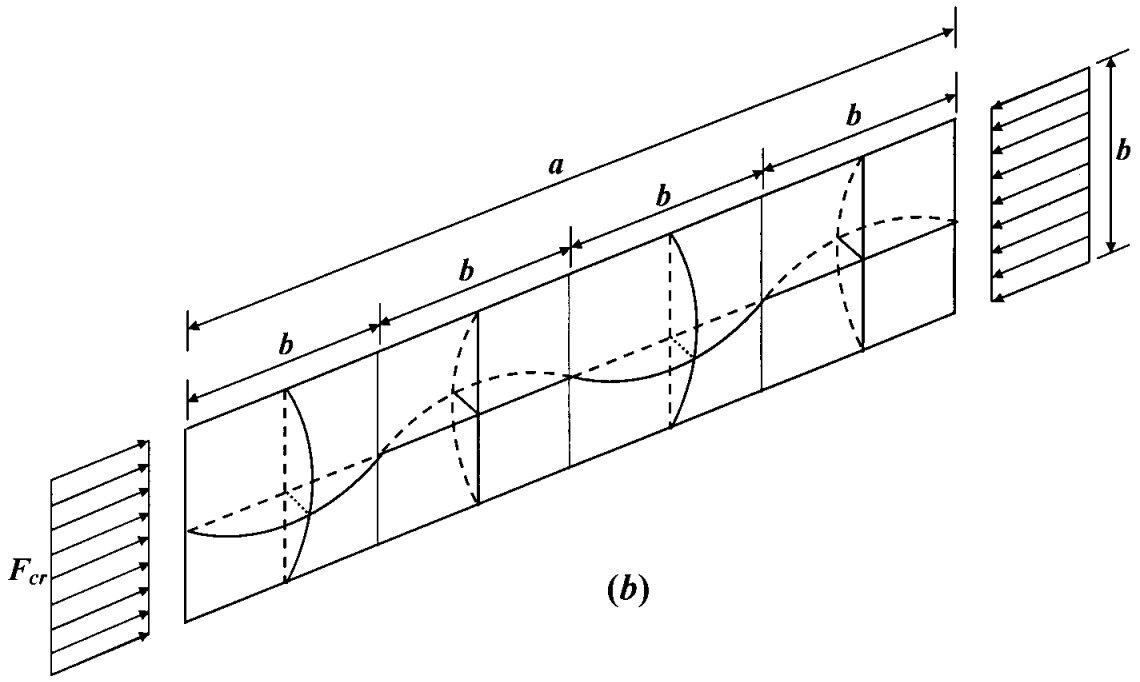

(*b*)

Figure W8.5.2: Buckling of a long thin rectangular plate under edge compression.

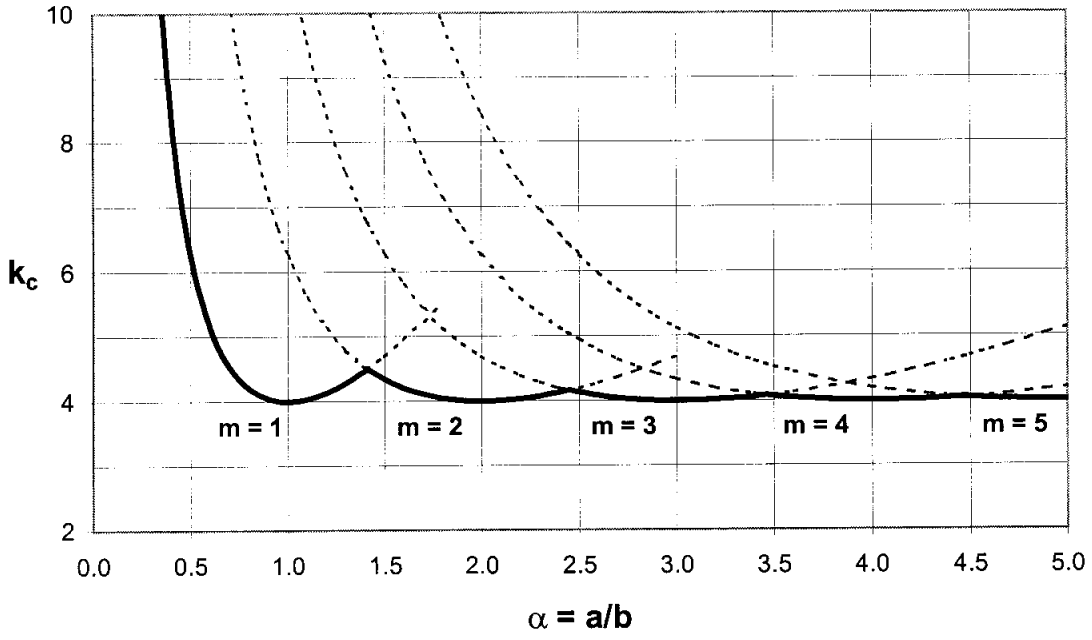

Figure W8.5.3: Buckling coefficients for a simply supported, rectangular flat plate under edge compression.